THE JOURNAL OF BIOLOGICAL CHEMISTRY
Vol. 278, No. 2, Issue of January 10, pp. 1059–1066, 2003

Printed in U.S.A.

ERdj5, an Endoplasmic Reticulum (ER)-resident Protein Containing DnaJ and Thioredoxin Domains, Is Expressed in Secretory Cells or following ER Stress*

Received for publication, July 12, 2002, and in revised form, October 25, 2002
Published, JBC Papers in Press, October 30, 2002, DOI 10.1074/jbc.M206995200

Paula M. Cunnea‡, Antonio Miranda-Vizuete‡§, Gloria Bertoli§¶, Thomas Simmen¶‖, Anastasios E. Damdimopoulos‡, Stefan Hermann, Saku Leinonen‡‡, Markku Pelto Huikko‡‡, Jan-Åke Gustafsson‡, Roberto Sitia¶§§¶¶, and Giannis Spyrou‡¶¶‖‖**

*From the ‡Centre for Biotechnology, Department of Biosciences at Novum, Karolinska Institute, and the **Steroid Group, Södertörns Högskola, S-14157 Huddinge, Sweden, ¶Department of Biological and Technological Research, San Raffaele Scientific Institute, and the §§Università Vita-Salute San Raffaele, 20132 Milan, Italy, and the ‡‡Department of Developmental Biology, Tampere University Medical School, and the Department of Pathology, Tampere University Hospital, Fin-33101 Tampere, Finland*

A complex array of chaperones and enzymes reside in the endoplasmic reticulum (ER) to assist the folding and assembly of and the disulfide bond formation in nascent secretory proteins. Here we characterize a novel human putative ER co-chaperone (ERdj5) containing domains resembling DnaJ, protein-disulfide isomerase, and thioredoxin domains. Homologs of ERdj5 have been found in *Caenorhabditis elegans* and *Mus musculus*. In *vitro* experiments demonstrated that ERdj5 interacts via its DnaJ domain with BiP in an ATP-dependent manner. ERdj5 is a ubiquitous protein localized in the ER and is particularly abundant in secretory cells. Its transcription is induced during ER stress, suggesting potential roles for ERdj5 in protein folding and translocation across the ER membrane.

The endoplasmic reticulum (ER)[1] is the site where membrane and secretory proteins fold, assemble, and form disulfide bonds. The ER provides a suitable environment for these processes, with optimal pH and redox conditions and a vast array of chaperones and enzymes available, including protein-disulfide isomerase (PDI), BiP (immunoglobulin heavy chain-binding protein), GRP94, and calnexin (1–3). The ER exerts also a tight quality control on its protein products; as a result, only proteins that attain their native state are transported to the Golgi. Proteins that fail to fold or assemble are dislocated to the cytosol for proteasomal destruction (4, 5). In both yeast and mammalian cells, the accumulation of misfolded polypeptides in the ER lumen results in the transcriptional up-regulation of many genes encoding ER-resident chaperones and folding catalysts, a process known as the unfolded protein response (UPR) (6, 7). Genes induced during the UPR share regulatory sequences, ER stress elements (ERSEs), or a UPR element (6, 8–10).

Like other members of the Hsp70 family, BiP interacts with newly synthesized polypeptides in ATP-dependent cycles of binding and release that are controlled by co-chaperone molecules of the DnaJ family. Because the intrinsic ATPase activity of Hsp70 proteins is weak (11), DnaJ molecules play a crucial role in catalyzing these reactions, stimulating the ATPase activity, and facilitating substrate binding (12, 13). DnaJ proteins can be divided into three subgroups based upon their degree of conservation in relation to *Escherichia coli* DnaJ. Type I DnaJ proteins contain an N-terminal J domain, a G/F-rich region, and a cysteine-rich Zn^{2+}-binding region. Type II DnaJ proteins lack the cysteine-rich domain, whereas type III proteins contain only the J domain (14). The latter mediates the interaction with the Hsp70 partner(s) via a conserved His-Pro-Asp motif.

Catalysis of oxidative folding is necessary to rapidly generate the correct disulfide bonds in newly synthesized proteins (15). A crucial component of the ER folding machinery is PDI. This multifunctional protein catalyzes disulfide bond formation and isomerization within the ER and displays both chaperone and anti-chaperone activities, depending on its redox state (15, 16). PDI needs to be continually reoxidized to be effective as a catalyst for disulfide bond formation. Members of the Ero1 family carry out this reoxidizing function in yeast and mammalian cells (17–19). The structure of PDI encompasses five domains: four consecutive domains (*a*-*b*-*b*′-*a*′) followed by a *c* region, which is a putative, low-affinity, high-capacity Ca^{2+}-binding site (15). The two C*XX*C protein-thiol oxidoreductase active sites are located in the *a* and *a*′ domains, which display homologies to thioredoxin (20). Despite their low sequence homology to the *a* domain, the *b* and *b*′ domains also adopt a thioredoxin fold. Therefore, PDI is assumed to be composed of redox active and inactive thioredoxin modules (20).

In addition to PDI, the ER contains numerous other proteins

* This work was supported in part by Swedish Medical Research Council Projects 13X-10370 and 19X-11622-03C and by grants from the Medical Research Fund of Tampere University Hospital, the Funds of University of Tampere, the Karolinska Institute, Södertörns Högskola, the Associazione Italiana per la Ricerca sul Cancro (AIRC), the Italian Ministry of University and Research (MIUR, Center of Excellence in Physiopathology of Cell Differentiation), PRIN (2002.058218_006), and Telethon (GP0117/01). The CELERA Database was used under, license agreement with the Karolinska Institute (Stockholm). The costs of publication of this article were defrayed in part by the payment of page charges. This article must therefore be hereby marked "*advertisement*" in accordance with 18 U.S.C. Section 1734 solely to indicate this fact.

The nucleotide sequence(s) reported in this paper has been submitted to the GenBank™/EBI Data Bank with accession number(s) AF038503 and AF255459.

§ Both authors contributed equally to this work.
‖ Recipient of a fellowship from Telethon (380/bs).
¶¶ Both authors contributed equally to this work.
‖‖ To whom correspondence should be addressed. Tel.: 46-8-608-9162; Fax: 46-8-774-5538; E-mail: giannis.spyrou@cbt.ki.se.

[1] The abbreviations used are: ER, endoplasmic reticulum; PDI, protein-disulfide isomerase; UPR, unfolded protein response; ERSE, endoplasmic reticulum stress element; EST, expressed sequence tag; RACE, rapid amplification of cDNA ends; GST, glutathione *S*-transferase; ORF, open reading frame; GFP, green fluorescent protein.

endowed with oxidoreductase activity (ERp72, ERp57, p5, etc.). The abundance of these proteins probably reflects the high demand for efficiently forming, isomerizing, and also reducing disulfide bonds in proteins that are undergoing folding and quality control in this organelle (21). The interactions between ERp57 and either calnexin or calreticulin underlie the necessity of coordinating folding with disulfide bond formation. We report here the identification and characterization of a novel ER-resident molecule (ERdj5) that features a DnaJ domain, a PDI-like domain, and a thioredoxin domain, suggesting a role as an ER folding assistant.

EXPERIMENTAL PROCEDURES

cDNA Cloning of Human ERdj5—BLAST (22) was used to identify human expressed sequence tag (EST) clones encoding proteins similar to thioredoxin. Some of these EST entries were found to encode a putative protein containing both a DnaJ domain and four putative thioredoxin-like active sites. Based on these sequences, the following primers were designed and used for 5′- and 3′-RACE/PCR in human testis and adrenal gland cDNA libraries (Clontech) to isolate human *ERdj5* cDNA: human ERdj5-F1 and ERdj5-F2, nucleotides 1960–1985 and 1344–1359, respectively (nucleotide numbers refer to GenBank™/EBI accession number AF038503); and human ERdj5-R1 and ERdj5-R2, nucleotides 2479–2455 and 2518–2482, respectively. The resulting sequences were used to amplify by PCR the full-length cDNA of *ERdj5* from the same libraries.

Glutathione S-Transferase (GST) Purification of the DnaJ Domain of ERdj5 and Full-length ERdj5—The DnaJ domain was amplified by PCR using primers ERdj5/GST-F1 (nucleotides 438–468) and ERdj5/GST-R1 (nucleotides 672–701), containing *Bam*HI and *Eco*RI restriction sites, respectively. The product was digested with *Bam*HI and *Eco*RI and cloned into the pGEX-4T-1 vector. A fusion protein between GST and the DnaJ domain of ERdj5 (GST-DnaJ) was purified from *E. coli* BL21(DE3) cells by growing a 250-ml culture to $A_{600} \sim 0.6$ and then inducing protein expression by adding 1 mM isopropyl-1-thio-β-D-galactopyranoside and incubating for an additional 4 h at 37 °C. Cells were pelleted by centrifugation. The pellet was resuspended in 12.5 ml of ice-cold buffer containing 20 mM Tris (pH 8), 50 mM NaCl, and 1 mM phenylmethylsulfonyl fluoride. 150 μl of lysozyme (50 mg/ml) was added, and the solution was left stirring on ice for 30 min. Bacteria were then placed on ice, and 0.1 M $MnCl_2$, 1 M $MgCl_2$, 1 mg/ml DNase, and 1 mg/ml RNase (150 μl each) were added and incubated for a further 45 min on ice. Bacteria were lysed by sonication, and the debris was removed by centrifugation at 15,000 rpm for 45 min at 4 °C. The supernatant was added to 2 ml of prepared glutathione slurry, and protein was eluted according to the manufacturer's recommendations (Amersham Biosciences).

Full-length *ERdj5* was amplified by PCR using the specific forward and reverse primers ERdj5/GST-F1 (see above) and ERdj5/GST-R2 (nucleotides 2727–2756), including *Bam*HI and *Sal*I restriction sites, respectively; digested; and cloned into the corresponding sites in the pGEX-4T-1 vector. GST-ERdj5 fusion protein was purified from *E. coli* BL21(DE3) cells according to the previously described protocol (23). GST-ERdj5 fusion protein was extensively dialyzed following purification.

Northern Blot Analysis—Human multiple-tissue Northern blots with poly(A)$^+$ RNA from different tissues were purchased from Clontech. The human *ERdj5* open reading frame (ORF) and the human PDI ORF were labeled with [α-^{32}P]dCTP (Rediprime random primer labeling kit, Amersham Biosciences) and hybridized at 65 °C overnight in ExpressHyb solutions following the protocol provided by Clontech. The blots were also hybridized with human β-actin as a control.

Green Fluorescent Protein (GFP) with ERdj5 Plasmid Generation—First, the pEGFP-N3 plasmid was modified so that the ER retention signal would be at the end of the GFP sequence. PCR was used with specially designed primers including the appropriate restriction sites, the stop codon, and the ER retention signal KDEL to amplify GFP-KDEL. This product was ligated into the pGEMT-easy plasmid and sequenced to confirm the presence of the KDEL sequence. The GFP DNA was released from the pEGFP-N3 plasmid by digestion with the restriction enzymes *Not*I and *Eco*RI. The modified GFP-KDEL was released from the pGEMT-easy plasmid by digestion with *Not*I and *Eco*RI and subsequently cloned into the empty pEGFP-N3 *Not*I and *Eco*RI sites (also sequenced to confirm KDEL presence). This modified plasmid (pEGFP-KDEL) was used for GFP localization studies. The *ERdj5* sequence not including the ER retention signal sequence (KDEL) was amplified using forward and reverse primers containing *Xho*I and *Bam*HI restriction sites, respectively, and the Kozak sequence (24). This *ERdj5* product was digested and ligated in-frame into pEGFP-KDEL.

Confocal Microscopy Localization Studies of GFP-tagged ERdj5—HEK293 cells were chosen for these studies, as they are epithelial kidney adherent cells that are easily transiently transfected. The 293 cell line is a permanent line of primary human embryonic kidney cells transformed by sheared human adenovirus type 5 DNA (American Type Culture Collection, Manassas, VA). HEK293 cells were grown in 1:1 Dulbecco's modified Eagle's medium/nutrient mixture F-12 supplemented with fetal calf serum and 10 μg/ml gentamycin and transiently transfected using polyethyleneimine (Aldrich). 1 μg of GFP- plus KDEL-tagged ERdj5 DNA and 1 μg of pDsRed2-ER (Clontech) DNA were diluted in 20 μl of H_2O, and 1 μl of 0.1 M polyethyleneimine was added. The mixture was vortexed, incubated at room temperature for 10 min, and subsequently added to the medium and applied to the cells. 48 h after transfection, live GFP pictures were acquired with a Leica laser scanning confocal microscope. GFP was excited at a wavelength of 488 nm using an argon/krypton laser, and emitted light was collected between 500 and 540 nm; and for excitation of pDsRed2-ER (Clontech), we used the 568-nm line, and emitted light was collected between 570 and 620 nm.

Generation and Purification of His-tagged BiP—The *BiP* cDNA including the signal peptide was amplified from a human liver cDNA library by PCR using the specific forward and reverse primers BiP-F5 (nucleotides 131–160) and BiP-R1 (nucleotides 2164–2180), corresponding to GenBank™/EBI accession number X87949 for *Homo sapiens BiP* mRNA. The product was ligated into the pGEMT-easy vector. To generate suitable restriction sites for cloning into the pET-15b plasmid for subsequent protein purification, PCR was carried out using primers BiP-pET-F (nucleotides 268–291) and BiP-pET-R (nucleotides 2167–2193), containing *Nde*I and *Bam*HI restriction sites, respectively, with pGEM-BiP cDNA as template. Following digestion with *Bam*HI and *Nde*I, the product was ligated in-frame into the His-tagged pET-15b plasmid (Novagen). His-tagged BiP was purified essentially following a previous protocol (25).

Surface Plasmon Resonance Interaction Studies—Surface plasmon resonance was carried out using a BIAcore2000 instrument (BIAcore, Uppsala, Sweden). Using amine coupling, anti-GST antibodies (~6000 response units) were immobilized onto all surfaces of a CM5 sensor chip (BIAcore). Subsequently, equal molar quantities of GST and the GST-DnaJ and GST-ERdj5 fusion proteins were captured. All proteins were diluted in HBS-EP (10 mM HEPES, pH 7.4, 150 mM NaCl, 3 mM EDTA, 0.005% polysorbate) (BIAcore) supplemented with 5 mM $MgCl_2$ and injected at a flow rate of 5 μl/min. The GST signal was used for background correction.

GST Pull-down Experiments with in Vitro Translated BiP and His-tagged BiP—The *BiP* ORF cloned into the pET-15b vector from the previous BiP protein purification was used as template for *in vitro* translation. Protein was synthesized *in vitro* using the T7 RNA polymerase-based rabbit reticulocyte lysate-coupled transcription/translation kit (TNT, Promega) and labeled with [^{35}S]Met. Briefly, GST, GST-DnaJ, and GST-ERdj5 (~2 μg each) bound to glutathione-Sepharose 4B beads were incubated for 2 h upon rotating at 4 °C with 4 μl of *in vitro* translated [^{35}S]Met-labeled protein in incubation buffer (50 mM potassium inorganic phosphate (pH 7.4), 100 mM NaCl, 1 mM $MgCl_2$, 10% glycerol, and 0.1% Tween) containing 1.5% bovine serum albumin. (As a control, GST and the GST fusion proteins were incubated under the same conditions without *in vitro* translated BiP protein.) The beads were washed three times for 15 min with incubation buffer without bovine serum albumin, resuspended in 100 μl of 2× SDS sample buffer, boiled for 5 min, and pelleted in a microcentrifuge. 15 μl of each supernatant was subjected to SDS-PAGE. To control the stability of the GST fusion proteins and equal loading, gels were stained with Coomassie Blue, incubated in Amplify liquid (Amersham Biosciences) for 15 min, and dried under vacuum before autoradiography.

GST pull-down assays using His-tagged BiP were carried out essentially as described above. Briefly, 2 μg of purified His-tagged BiP protein was added to ~2 μg of GST, GST-DnaJ, or GST-ERdj5 bound to glutathione-Sepharose 4B beads in the presence of 2 mM ATP or ADP and incubated overnight at 4 °C. Following SDS-PAGE, proteins were transferred to Hybond-C super membrane (Amersham Biosciences) using standard Western blotting techniques. Monoclonal anti-His tag antibody (Clontech) was used at a dilution of 1:2000 with horseradish peroxidase-linked sheep anti-mouse Ig (Amersham Biosciences) used as the secondary antibody at a dilution of 1:5000.

In Situ Hybridization of Mouse ERdj5—For *in situ* hybridization,

adult male and female mice (2–3 months of age) were killed with carbon dioxide, and the tissues were excised and frozen on dry ice. The samples were sectioned with a Microm HM500 cryostat at 14 μm and thaw-mounted onto polylysine glass slides (Menzel). The sections were stored at −20 °C until used. Four oligonucleotide probes for the ORF of mouse *ERdj5* (nucleotides 329–356, 543–582, 1269–1303, and 2232–2269, GenBank™/EBI accession number AF255459) were used and labeled to a specific activity of 1×10^9 cpm/μg with [α-^{33}P]dATP (PerkinElmer Life Sciences) using terminal deoxynucleotidyltransferase (Amersham Biosciences). The probe sequences exhibit <60% similarity to all known sequences in the GenBank™/EBI Data Bank. All probes gave similar expression results when used separately and were usually combined to intensify the hybridization signal. As a control for the specificity of *in situ* hybridizations, several probes for unrelated mRNAs with known expression patterns and with similar lengths and GC contents were used. The addition of a 100-fold excess of the respective unlabeled probe abolished all hybridization signals. *In situ* hybridization was carried out as described previously (26).

ERdj5 mRNA Expression and UPR Induction—HEK293T cells (American Type Culture Collection), an easily transfectable derivative of HEK293 cells expressing SV40 T antigen, were grown in Dulbecco's modified Eagle's medium with 5% fetal calf serum. Total cellular RNA preparation and Northern blot analysis were carried out as described previously (27). To induce the UPR or unrelated stress response, cells were cultured for 6 h in the presence of dithiothreitol (2 mM), tunicamycin (10 μg/ml), thapsigargin (2 μM), A23187 (2 μM), EGTA (2 mM), or deoxyglucose (10 mM); deprived of fetal calf serum; UV light-irradiated; or incubated at 42 °C for 30 min.

RESULTS

cDNA Cloning of ERdj5 and Sequence Analysis—A screen of the GenBank™/EBI EST Data Bank led to the identification of sequences containing putative thioredoxin active sites. 5′- and 3′-RACE/PCR analyses were performed using specially designed primers in both human testis and adrenal gland cDNA libraries to clone the full-length cDNA. The PCR product was cloned and sequenced, confirming the sequence obtained from the ESTs. The complete sequence reveals an ORF of 2379 base pairs, with 5′- and 3′-untranslated regions of 415 and 1384 base pairs, respectively, surrounding an ORF that encodes a putative protein of 793 amino acids with an estimated molecular mass of 91 kDa and a pI of 7.03 (Fig. 1). The protein was named ERdj5 following the nomenclature proposed for ER proteins containing a DnaJ domain in the recent study by Shen *et al.* (28). After an N-terminal hydrophobic sequence, a domain with the features of DnaJ/Hsp40 proteins, including the His-Pro-Asp motif, is encountered (Fig. 2*A*). Neither G/F-rich nor cysteine-rich regions are present, thus making ERdj5 a type III DnaJ protein (14, 29). Following the DnaJ domain are four thioredoxin-like domains, with different putative redox active sites, each containing a C*XX*C motif. The last domain has a typical thioredoxin signature, WCGPC. A KDEL tetrapeptide is present at the C terminus, possibly mediating ER retention (see below).

Genomic Organization and Chromosomal Localization of ERdj5—The gene encoding *ERdj5* has been identified in genomic data bases and mapped to human chromosome 2 at positions p22.1–23.1. Several disease genes have been mapped to this region, including a form of recessive deafness and some types of colon cancer. Using the CELERA Database, we were able to decipher the genomic organization of the *ERdj5* gene. It spans ~62 kb and is composed of 24 exons (Fig. 2*B*). Splicing variants were detected both in ESTs and in cDNAs. Homologs of human *ERdj5* are present in both *Mus musculus* and *Caenorhabditis elegans* (Fig. 1).

Tissue Distribution of ERdj5—Human multiple-tissue Northern blots were used to determine transcript size and distribution using the *ERdj5* ORF as a probe. Signals were detected in all tissues analyzed; their distribution was similar to that of PDI mRNAs, being particularly abundant in secretory organs (Fig. 3). Multiple *ERdj5* bands, possibly representing splicing variants, were identified in the pancreas and testis, with bands of less intensity identified in the heart, liver, spleen, prostate, and ovary and weaker bands seen in the rest of the tissue panel. A similar pattern was confirmed using the virtual tissue distribution program.[2]

Expression of ERdj5 in Secretory Tissues—In situ hybridization was employed to further analyze the distribution of *ERdj5* transcripts in mice. The results shown in Fig. 4 confirm that *ERdj5* transcripts are particularly abundant in secretory tissues. Thus, the adrenal gland showed very strong signals in the cortex and medulla (Fig. 4*A*). Expression in the nervous system was variable. Strong signals were found in several areas of the central nervous system, particularly in the hippocampus and the granular cell layer of the cerebellar cortex (Fig. 4*B*). Moderate signals were seen in the cerebral cortex, olfactory bulb, striatum, hypothalamus, and brain stem, whereas the thalamus showed lower expression. White matter was negative. A strong signal was present in the ependyma covering the ventricles and plexus choroideus (Fig. 4*B*). In the spinal cord, there was a moderate signal in the gray matter, but the signal was absent in the white matter. In the peripheral nervous system, a strong signal was evident in the sympathetic (superior cervical) and sensory (trigeminal) ganglia (Fig. 4*C*). From emulsion autoradiography, it was apparent that the signal was present in the neurons, but absent in the glial cells (Fig. 4*D*). *ERdj5* mRNAs were abundant in genital organs. The epididymis showed a strong signal in the epithelium (Fig. 4*E*). The prostate expressed *ERdj5* at the highest level of all organs studied (Fig. 4*F*). In dipped sections, the signal was restricted to the epithelium (Fig. 4*G*). Also the alimentary tract expressed *ERdj5* in several areas. In the tongue, the stratified epithelium showed moderate labeling, whereas the striated muscle was not labeled (Fig. 4*H*). In the oral cavity, the epithelium and sublingual salivary glands were strongly labeled (Fig. 4*I*). In the esophagus (Fig. 4*J*) and larynx (Fig. 4*K*), the signal was particularly intense in the mucosa and mucous glands, respectively. Throughout the intestinal canal, from the stomach to the colon, a strong signal was seen in the mucosa, whereas the smooth muscle layer was negative (Fig. 4*L*).

ERdj5 Is Localized to the ER—The presence of an N-terminal hydrophobic sequence and a C-terminal KDEL motif suggests that ERdj5 is an ER-resident protein. Indeed, a chimeric protein in which GFP was inserted immediately before the KDEL sequence of ERdj5 displayed a reticular pattern, largely coinciding with the ER marker used, pDsRed-ER (Fig. 5). Also, Myc-tagged ERdj5 was localized in the ER of HeLa transfectants.[3]

ERdj5 Interacts with BiP via the DnaJ Domain—Hsp70 members have been shown to interact *in vitro* with GST fusion proteins containing their J domain protein partners (2, 25, 30–32). To investigate whether the DnaJ domain of ERdj5 can interact with BiP, we used surface plasmon resonance assays (33). Either full-length ERdj5 or its DnaJ domain fused with GST was immobilized in separate channels on a BIAcore CM5 chip (see "Experimental Procedures"). Binding to BiP was then tested in the presence of ATP and ADP. In the presence of ATP, the BiP protein bound to both GST-DnaJ and GST-ERdj5. No binding to the control channel containing the GST protein alone was observed. As expected, there was no binding in the presence of ADP or in the absence of either ATP or ADP. To further confirm the binding of ERdj5 and its DnaJ domain to BiP, *in vitro* GST pull-down experiments were carried out (Fig. 6, *B* and *C*). *In vitro* translated BiP bound to GST-DnaJ and

[2] Available at www.labonweb.com.

[3] T. Simmen, G. Bertoli, and R. Sitia, unpublished data.

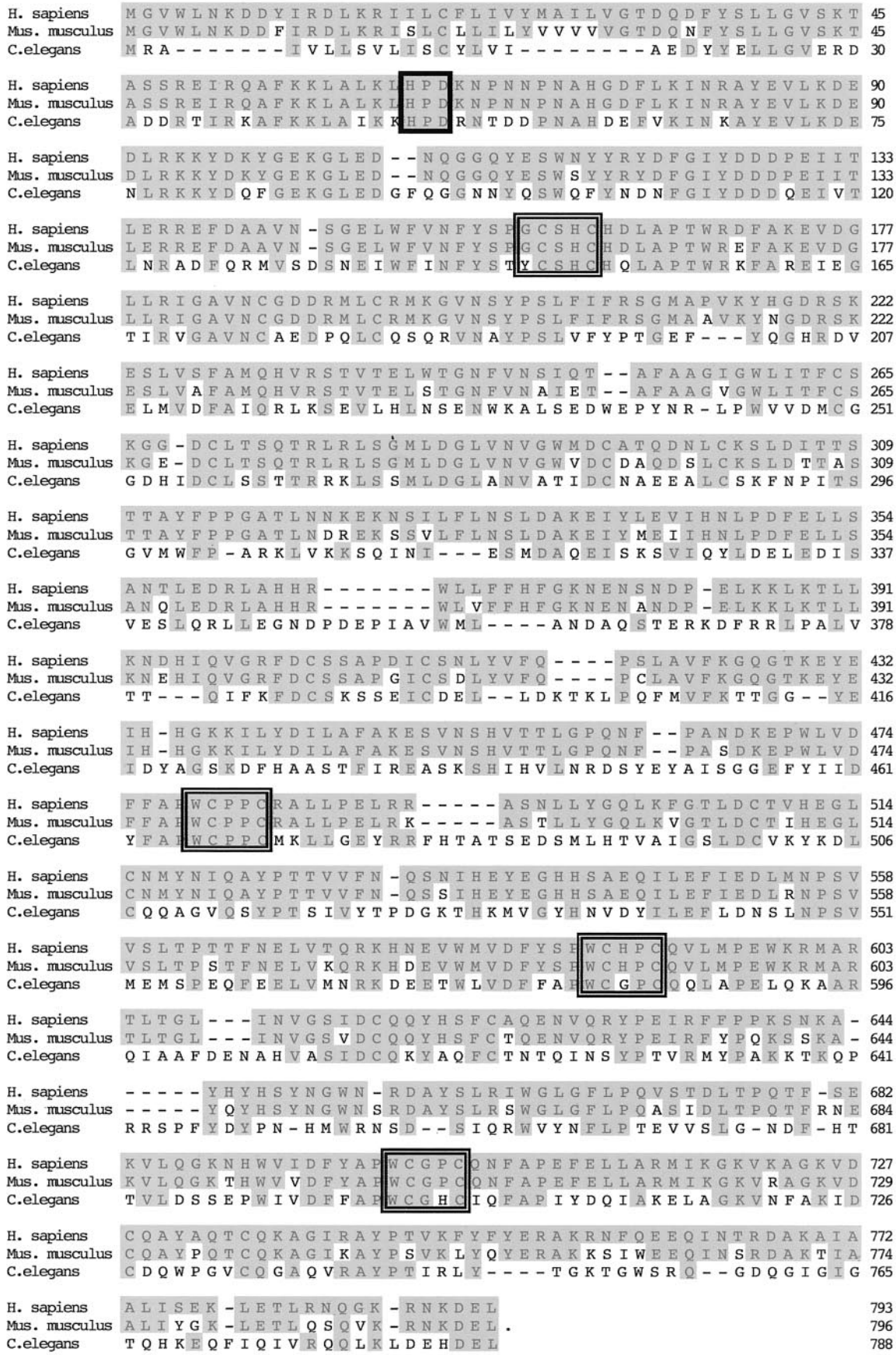

FIG. 1. **Homology alignment of human ERdj5 with *C. elegans* and *M. musculus* ERdj5.** Shown is a comparison of the derived human ERdj5 sequence with the *M. musculus* and *C. elegans* homologs identified in the *M. musculus* and *C. elegans* genome data bases, respectively. *Gray boxes* indicate amino acid matches. Within the protein sequence of ERdj5, the tripeptide His-Pro-Asp conserved in all DnaJ proteins is surrounded with a *single-lined box*, and the four putative thioredoxin domains are highlighted with *double-lined boxes*.

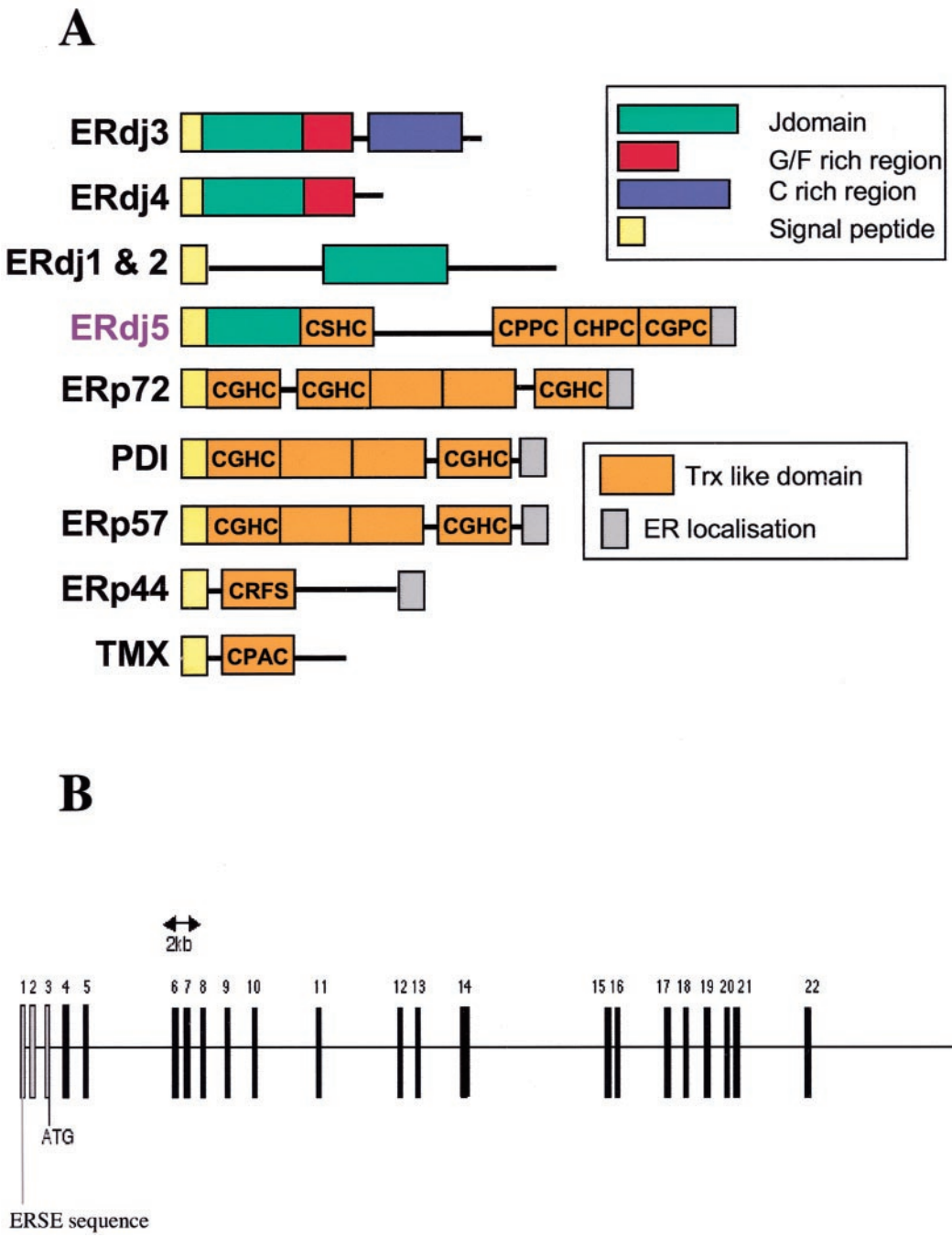

FIG. 2. **Genomic and domain organization of ERdj5.** *A*, ERdj5 is an ER-resident protein containing DnaJ-, thioredoxin (*Trx*)-, and PDI-like domains. In the scheme, DnaJ proteins are classified based on the presence of a J domain, a G/F-rich region, and a cysteine-rich region. Classification of thioredoxin-like domains is based on sequence similarity of their putative active sites to the thioredoxin or PDI C*XX*C motif. *B*, genomic organization of human the *ERdj5* gene. The 24 exons of human *ERdj5* (represented by *numbered gray* and *black bars*) are distributed over ~62 kb of chromosome 2 at p22.1–23.1. Exons 1–3 (*gray bars*) are composed of the 5′-untranslated region, with the ORF starting in exon 3. Exon 24 (*gray bar*) contains the stop codon plus the 3′-untranslated region.

GST-ERdj5, but not to GST (Fig. 6*B*). Likewise, both GST-ERdj5 and GST-DnaJ bound to purified His-tagged BiP. Binding was more efficient in the presence of ATP (Fig. 6*C*).

ERdj5 Is Up-regulated upon ER Stress—The accumulation of unfolded proteins in the ER activates the UPR, thus inducing the transcription of many ER-resident chaperones. We examined whether ERdj5 is also up-regulated in times of ER stress. Following treatment of HEK293T cells with a panel of common UPR inducers as previously described (34, 35), ERdj5 transcription was up-regulated (Fig. 7). Heat shock and serum deprivation resulted in no induction, suggesting that *ERdj5* is a *bona fide* UPR gene. This correlates with the presence of an ERSE-like box ($CCAATN_9CGCGG$) ~330 bases upstream of the *ERdj5* ATG start codon, with N_9 consisting of mainly guanine and cytosine nucleotides, which is common for ERSE motifs. The ERdj5 pattern of up-regulation following stress is similar to that seen for *Ero1-Lβ*, which is a known UPR gene (35).

DISCUSSION

We describe here a novel human ER-resident protein (ERdj5) ubiquitously expressed and abundant in secretory tissues such as pancreas and testis. Homologs of human *ERdj5* are present in both *M. musculus* and *C. elegans*. The presence of DnaJ-,

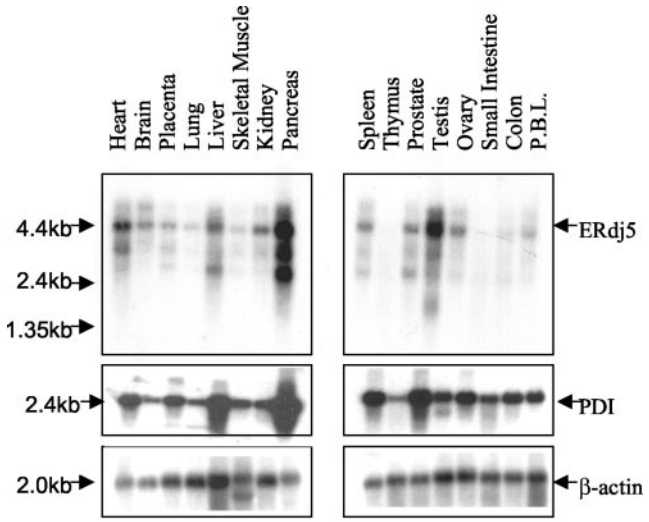

FIG. 3. **Detection of *ERdj5* mRNA expression in human tissues by RNA hybridization.** A blot containing 2 μg of polyadenylated RNA from human tissues was hybridized with radiolabeled *ERdj5* cDNA, PDI cDNA, or β-actin probes. The migration positions of molecular mass markers are indicated. *P.B.L.*, peripheral blood leukocytes.

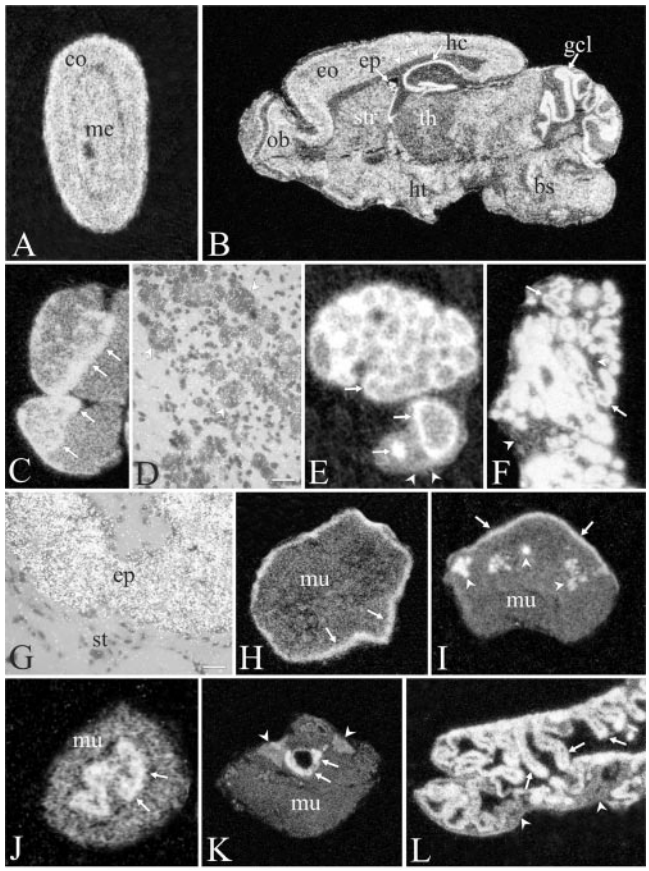

FIG. 4. **Demonstration of *ERdj5* mRNA in mouse tissues by *in situ* hybridization.** *A*, strong signals for *ERdj5* are seen in the cortex (*co*) and medulla (*me*) of the adrenal gland. *B*, the sagittal section of the brain shows strong signals in the hippocampus (*hc*), the granular layer of the cerebellar cortex (*gcl*), and the ependyma (*ep*) in ventricles. Moderate expression is seen in the olfactory bulb (*ob*), cerebral cortex (co), striatum (*str*), hypothalamus (*ht*), and brain stem (*bs*). A weak signal is present in the thalamus (*th*), whereas the white matter (corpus callosum indicated by *arrowheads*) is not labeled. *C*, a strong signal is shown in the neurons of trigeminal ganglia (*arrows*), but is absent in glial cells. *D*, a dipped section shows a signal in the neurons of the trigeminal ganglion (*arrowheads*). *Bar* = 40 μm. *E*, in the epididymis, a strong signal is present in the epithelium (*arrows*), whereas stroma (*arrowheads*) is unlabeled. *F*, an extremely strong signal is seen in the epithelium of the prostate (*arrows*), whereas the stroma (*arrowheads*) is negative. *G*, a dipped section shows a strong signal in the epithelium (*ep*) of the prostate, whereas stromal (*st*) fibroblasts and smooth muscle cells are unlabeled. *Bar* = 15 μm. *H*, the stratified squamous epithelium (*arrows*) of the tongue is clearly labeled, whereas striated muscle (*mu*) is unlabeled. *I*, in the floor of the oral cavity, the epithelium (*arrows*) and the sublingual salivary glands (*arrowheads*) are intensely labeled. *mu*, muscle. *J*, the epithelium of the esophagus (*arrows*) is labeled, whereas the smooth muscle layer (*mu*) is negative. *K*, the mucous glands of the larynx (*arrows*) are strongly positive, whereas the thyroid glands (*arrowheads*) are weakly labeled, and the muscles (*mu*) are unlabeled. *L*, a strong signal is seen in the mucosa (*arrows*) of the colon, whereas the muscle layer (*arrowheads*) is unlabeled.

PDI-, and thioredoxin-like domains suggests that ERdj5 may be involved in assisting protein folding and quality control in the ER. Several lines of evidence including the transcriptional regulation of *ERdj5* and its subcellular localization and molecular interactions support this hypothesis. The presence of an N-terminal leader sequence and a C-terminal KDEL motif confirm our findings that ERdj5 is localized in the ER. GFP-tagged ERdj5 with the ER retention signal KDEL yields a reticular staining pattern, largely superimposable on that obtained with ER markers.

As in the case of many other proteins induced during the UPR, the *ERdj5* promoter contains a putative ERSE box (9). This correlates with the observation that tunicamycin, dithiothreitol, and thapsigargin and other common UPR inducers, but not cell stress inducers such as heat shock, UV light, and serum deprivation, induced the accumulation of *ERdj5* transcripts in HEK293T cells. The fact that *ERdj5* transcripts were not so highly induced could reflect the presence of a single ERSE-like box, whereas other ER chaperones such as BiP have multiple ERSE boxes and are usually very highly induced upon ER stress (9, 19, 34). In HEK293T cells, all *ERdj5* transcripts were induced to a lesser extent than *Ero1-Lβ* or *BiP* (34–35). The physiological significance of this difference deserves further investigation.

DnaJ proteins normally work in tandem with an Hsp70 partner, stimulating cycles of ATP hydrolysis and thus allowing Hsp70 proteins to bind and release substrates (36, 37). The human ER-resident Hsp70 protein BiP is no exception. Two DnaJ domain proteins (HEDJ and ERdj4) have recently been shown to bind to BiP and to stimulate its ATPase activity *in vitro*, respectively (25, 28). Our results show that also ERdj5 could be involved in this folding cycle via an interaction with BiP. Indeed, either full-length ERdj5 or its DnaJ domain alone can bind BiP in an ATP-dependent manner. Lack of ATP or substitution with ADP resulted in little or no interaction, suggesting that ERdj5 could function as a DnaJ cofactor for BiP.

The most intriguing feature of ERdj5 is the presence of DnaJ-, thioredoxin-like, and PDI-like domains on the same polypeptide backbone. Why does ERdj5 contain domains posed for different redox functions? And why are they linked to a DnaJ domain? The majority of membrane and secretory cargo proteins contain disulfide bonds that are often essential to attain the native state. Disulfide bond formation and disulfide isomerization occur in the ER and are catalyzed by an array of resident oxidoreductases, the prototype of which is PDI. In addition, disulfide bonds are reduced in the ER lumen prior to the dislocation of proteins destined to degradation (38, 39). Redox regulation in the ER must hence be precisely orchestrated (21). PDI functions as a catalyst in the oxidation and isomerization of disulfides on nascent polypeptides undergoing folding in the oxidizing environment of the ER (1). Recently, this oxidoreductase has also been involved in the dislocation of short-lived proteins targeted to proteasomal destruction (40, 41). Members of the thioredoxin/PDI families invariably con-

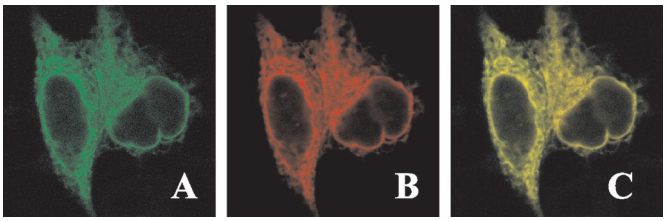

FIG. 5. **ERdj5 is an ER-resident protein.** *A*, HEK293 cells were transiently transfected with pEGFP-ERdj5, encoding the ORF of *ERdj5* fused to GFP with the endogenous ER KDEL at the C terminus. *B*, pDsRed2-ER (Clontech) was used as an ER localization control. *C*, the merging of *A* and *B* shown.

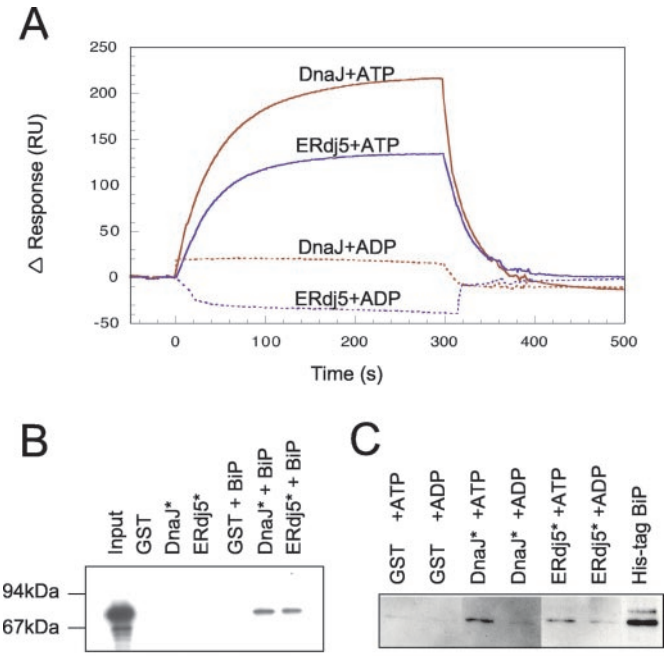

FIG. 6. **ATP-dependent binding of ERdj5 to BiP.** *A*, BIAcore interaction studies of BiP with ERdj5 and its DnaJ domain. BiP was diluted to a final concentration of 100 μM in HBS-EP supplemented with 5 mM $MgCl_2$ and either 5 mM ATP (*solid lines*) or 5 mM ADP (*broken lines*) and immediately analyzed for binding to DnaJ (*red*) and ERdj5 (*blue*) by surface plasmon resonance. *B*, *in vitro* translated BiP binds to ERdj5 and the DnaJ domain. GST pull-down experiments were performed to show the interaction between purified GST-ERdj5 or GST-DnaJ and *in vitro* translated BiP protein. *Asterisks* indicate GST-tagged proteins. The *first lane* contains 10% of the input of *in vitro* translated BiP that was added to the GST-tagged proteins. The *second* through *fourth lanes* contain GST protein and GST-tagged protein without the addition of *in vitro* translated BiP. The *fifth* through *seventh lanes* contain *in vitro* translated BiP added to the GST and GST-tagged proteins. *C*, ATP facilitates the binding of purified His-tagged BiP to the DnaJ domain of ERdj5. Purified His-tagged BiP (2 μg) was incubated with GST, GST-DnaJ, or GST-ERdj5 in the presence of 2 mM ATP or ADP as indicated. The *seventh lane* shows 4% of the His-tagged BiP input.

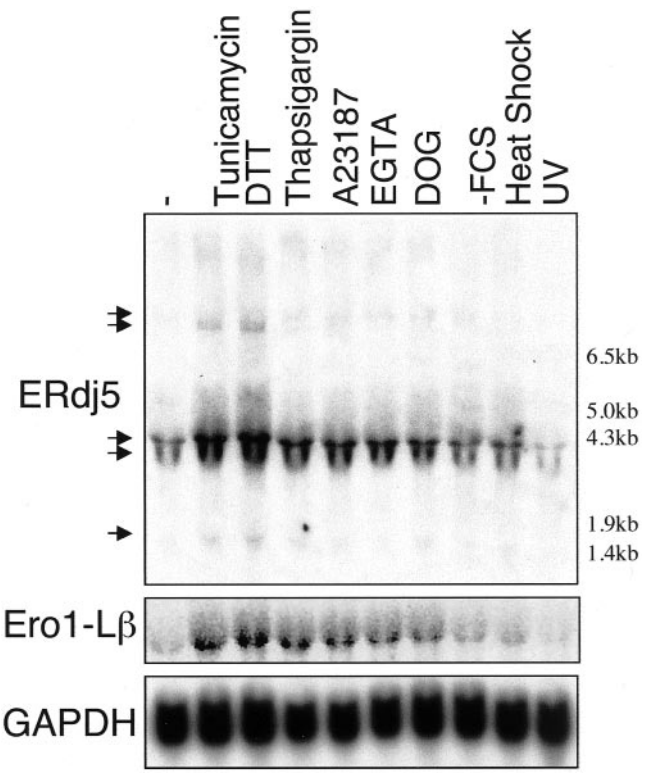

FIG. 7. ***ERdj5* transcripts are up-regulated upon ER stress.** HEK293T cells were treated with a number of stress-inducing drugs and conditions. Blots were hybridized with probes specific for *ERdj5*, *Ero1-Lβ* (35), and glyceraldehyde-3-phosphate dehydrogenase (*GAPDH*) as indicated. *Arrows* indicate possible splicing variants. *DTT*, dithiothreitol; *DOG*, deoxyglucose; *FCS*, fetal calf serum.

tain a C*XX*C motif. The redox activity of these proteins is dictated by the local pK of the relevant thiols groups, which in turn depends on the flanking amino acids. Thioredoxin, which normally acts as a reductase in the cytosol, can be turned into an oxidase by transplanting the intervening amino acids with those normally found in PDI (42, 43).

An important question remains concerning ERdj5: will it work as a thioredoxin, a PDI-like protein, or simply as a DnaJ partner for a corresponding Hsp70 or as a combination of all three? Using the standard thioredoxin activity assays of insulin reduction (44, 45), we have so far been unable to show any activity for recombinant ERdj5 (data not shown). However, this does not exclude that ERdj5 can act as a reductase on other substrates. Further analysis is ongoing to determine the thioredoxin activity of each of the four C*XX*C domains.

There are at least two main folding pathways that a nascent glycoprotein may select upon entry into the ER. One utilizes calnexin and calreticulin as chaperones; the other is based primarily on BiP. Calnexin and calreticulin have been shown to associate with ERp57, an oxidoreductase that shares extensive similarities with PDI (46), but does not seem to utilize Ero1 to be reoxidized (47). ERp57 plays a key role in the folding of class I major histocompatibility complex molecules (48). The calnexin-ERp57 partnership provides a dual specialization to nascent proteins that engage in this pathway, the former acting as a chaperone and the latter as an oxidoreductase. How does the BiP pathway handle the making of disulfide bonds in its client proteins? In yeast, BiP and PDI seem to interact with each other (49), perhaps forming a complex not dissimilar from the calnexin-ERp57 duo. The interaction we detected between BiP and the ERdj5 DnaJ domain is bound to bring the redox active domains of the latter in the vicinity of the main ER chaperone. Furthermore, a cooperative relationship between BiP and PDI has previously been shown *in vitro* in the oxidative folding of antibodies (50). It was hypothesized that in the absence of BiP, unfolded antibody chains collapse rapidly upon refolding, leaving the cysteine side chains inaccessible to PDI; but that in the presence of BiP, BiP binds the unfolded polypeptide chains and keeps them in a suitable conformation for PDI accessibility (50). Perhaps this is also the case for ERdj5. Its DnaJ domain could stimulate the ATPase activity of BiP, allowing BiP to bind unfolded polypeptide, thus leaving the cysteine residues of the polypeptide available for ERdj5.

Proteins that do not mature properly are retained in the ER and are eventually targeted for ER-associated degradation through the action of chaperones (51). Release from BiP is

essential for substrates to attempt productive folding as well as to be dislocated across the ER membrane for proteasomal destruction. During acute ER stress, detachment of substrates from chaperones may cause protein aggregation. In yeast, however, the UPR is intimately connected with the pathways of ER-associated degradation (7, 52). The thioredoxin-like domain present in ERdj5 might provide the reductive force that seems to be necessary to complete unfolding of proteins targeted for dislocation. It may also be important in reducing PDI so as to allow its function as an isomerase and in promoting dislocation (40). On the other hand, the additional domains (more similar to PDI) may enable ERdj5 to act on a wider range of substrates.

Despite the control mechanisms that exist in the ER, there are many diseases that are attributed to the misfolding or aggregation of proteins within the ER, *e.g.* Alzheimer's disease, prion-associated disorders, cystic fibrosis, etc. (53–56). ERdj5 is expressed in the neuronal cells of the hippocampus (*in situ* data not shown), which is a site of neuron degeneration in the brains of Alzheimer's disease patients. Perhaps ERdj5 also has a role in these misfolding disease states. Determining the precise function of ERdj5 and establishing whether the BiP-ERdj5 duo is important in the folding pathway or in the unfolding that is a prelude to dislocation deserve further investigation.

Acknowledgments—We thank Cristina Benedetti and Ineke Braakman for helpful reagents and suggestions. The excellent technical assistance of Ulla-Margit Jukarainen is greatly appreciated.

REFERENCES

1. Noiva, R. (1999) *Semin. Cell Dev. Biol.* **10,** 481–493
2. Brooks, D. A. (1999) *Semin. Cell Dev. Biol.* **10,** 441–442
3. Fink, A. L. (1999) *Physiol. Rev.* **79,** 425–449
4. Xiong, X., Chong, E., and Skach, W. R. (1999) *J. Biol. Chem.* **274,** 2616–2624
5. Kopito, R. R. (1997) *Cell* **88,** 427–430
6. Mori, K. (2000) *Cell* **101,** 451–454
7. Travers, K. J., Patil, C. K., Wodicka, L., Lockhart, D. J., Weissman, J. S., and Walter, P. (2000) *Cell* **101,** 249–258
8. Lee, A. S. (2001) *Trends Biochem. Sci.* **26,** 504–510
9. Yoshida, H., Haze, K., Yanagi, H., Yura, T., and Mori, K. (1998) *J. Biol. Chem.* **273,** 33741–33749
10. Kohno, K., Normington, K., Sambrook, J., Gething, M. J., and Mori, K. (1993) *Mol. Cell. Biol.* **13,** 877–890
11. Kelley, W. L. (1998) *Trends Biochem. Sci.* **23,** 222–227
12. Liberek, K., Marszalek, J., Ang, D., Georgopoulos, C., and Zylicz, M. (1991) *Proc. Natl. Acad. Sci. U. S. A.* **88,** 2874–2878
13. Misselwitz, B., Staeck, O., and Rapoport, T. A. (1998) *Mol. Cell* **2,** 593–603
14. Cheetham, M. E., and Caplan, A. J. (1998) *Cell Stress Chaperones* **3,** 28–36
15. Ferrari, D. M., and Soling, H. D. (1999) *Biochem. J.* **339,** 1–10
16. Freedman, R. B., Hirst, T. R., and Tuite, M. F. (1994) *Trends Biochem. Sci.* **19,** 331–336
17. Frand, A. R., and Kaiser, C. A. (1999) *Mol. Cell* **4,** 469–477
18. Tu, B. P., Ho-Schleyer, S. C., Travers, K. J., and Weissman, J. S. (2000) *Science* **290,** 1571–1574
19. Anelli, T., Alessio, M., Mezghrani, A., Simmen, T., Talamo, F., Bachi, A., and Sitia, R. (2002) *EMBO J.* **21,** 835–844
20. Sun, X., Dai, Y., Liu, H., Chen, S., and Wang, C. (2000) *Biochim. Biophys. Acta* **1481,** 45–54
21. Fassio, A., and Sitia, R. (2002) *Histochem. Cell Biol.* **117,** 151–157
22. Altschul, S. F., Madden, T. L., Schaffer, A. A., Zhang, J., Zhang, Z., Miller, W., and Lipman, D. J. (1997) *Nucleic Acids Res.* **25,** 3389–3402
23. Frangioni, J. V., and Neel, B. G. (1993) *Anal. Biochem.* **210,** 179–187
24. Kozak, M. (1996) *Mamm. Genome* **7,** 563–574
25. Yu, M., Haslam, R. H., and Haslam, D. B. (2000) *J. Biol. Chem.* **275,** 24984–24992
26. Konenen, J., and Pelto-Huikko, M. (1997) *Technical Tips Online* http://www.tto.trends.com/
27. Cabibbo, A., Consalez, G. G., Sardella, M., Sitia, R., and Rubartelli, A. (1998) *Oncogene* **16,** 2935–2943
28. Shen, Y., Meunier, L., and Hendershot, L. M. (2002) *J. Biol. Chem.* **277,** 15947–15956
29. Cyr, D. M., Langer, T., and Douglas, M. G. (1994) *Trends Biochem. Sci.* **19,** 176–181
30. Holstein, S. E., Ungewickell, H., and Ungewickell, E. (1996) *J. Cell Biol.* **135,** 925–937
31. Misselwitz, B., Staeck, O., Matlack, K. E., and Rapoport, T. A. (1999) *J. Biol. Chem.* **274,** 20110–20115
32. Suh, W. C., Lu, C. Z., and Gross, C. A. (1999) *J. Biol. Chem.* **274,** 30534–30539
33. Fagerstam, L. G., Frostell, A., Karlsson, R., Kullman, M., Larsson, A., Malmqvist, M., and Butt, H. (1990) *J. Mol. Recognit.* **3,** 208–214
34. Benedetti, C., Fabbri, M., Sitia, R., and Cabibbo, A. (2000) *Biochem. Biophys. Res. Commun.* **278,** 530–536
35. Pagani, M., Fabbri, M., Benedetti, C., Fassio, A., Pilati, S., Bulleid, N. J., Cabibbo, A., and Sitia, R. (2000) *J. Biol. Chem.* **275,** 23685–23692
36. Nishikawa, S., and Endo, T. (1997) *J. Biol. Chem.* **272,** 12889–12892
37. Corsi, A. K., and Schekman, R. (1997) *J. Cell Biol.* **137,** 1483–1493
38. Tortorella, D., Story, C. M., Huppa, J. B., Wiertz, E. J., Jones, T. R., Bacik, I., Bennink, J. R., Yewdell, J. W., and Ploegh, H. L. (1998) *J. Cell Biol.* **142,** 365–376
39. Fagioli, C., Mezghrani, A., and Sitia, R. (2001) *J. Biol. Chem.* **276,** 40962–40967
40. Tsai, B., Rodighiero, C., Lencer, W. I., and Rapoport, T. A. (2001) *Cell* **104,** 937–948
41. Tsai, B., Ye, Y., and Rapoport, T. A. (2002) *Nat. Rev. Mol. Cell. Biol.* **3,** 246–255
42. Krause, G., Lundstrom, J., Barea, J. L., Pueyo de la Cuesta, C., and Holmgren, A. (1991) *J. Biol. Chem.* **266,** 9494–9500
43. Mossner, E., Huber-Wunderlich, M., and Glockshuber, R. (1998) *Protein Sci.* **7,** 1233–1244
44. Spyrou, G., Enmark, E., Miranda-Vizuete, A., and Gustafsson, J.-Å (1997) *J. Biol. Chem.* **272,** 2936–2941
45. Wollman, E. E., d'Auriol, L., Rimsky, L., Shaw, A., Jacquot, J. P., Wingfield, P., Graber, P., Dessarps, F., Robin, P., and Galibert, F. (1988) *J. Biol. Chem.* **263,** 15506–15512
46. Freedman, R. B., Klappa, P., and Ruddock, L. W. (2002) *EMBO Rep.* **3,** 136–140
47. Mezghrani, A., Fassio, A., Benham, A., Simmen, T., Braakman, I., and Sitia, R. (2001) *EMBO J.* **20,** 6288–6296
48. Dick, T. P., Bangia, N., Peaper, D. R., and Cresswell, P. (2002) *Immunity* **16,** 87–98
49. Gillece, P., Luz, J. M., Lennarz, W. J., de la Cruz, F. J., and Romisch, K. (1999) *J. Cell Biol.* **147,** 1443–1456
50. Mayer, M., Kies, U., Kammermeier, R., and Buchner, J. (2000) *J. Biol. Chem.* **275,** 29421–29425
51. Ellgaard, L., Molinari, M., and Helenius, A. (1999) *Science* **286,** 1882–1888
52. Friedlander, R., Jarosch, E., Urban, J., Volkwein, C., and Sommer, T. (2000) *Nat. Cell. Biol.* **2,** 379–384
53. Taguchi, J., Fujii, A., Fujino, Y., Tsujioka, Y., Takahashi, M., Tsuboi, Y., Wada, I., and Yamada, T. (2000) *Acta Neuropathol.* **100,** 153–160
54. Chai, Y., Koppenhafer, S. L., Bonini, N. M., and Paulson, H. L. (1999) *J. Neurosci.* **19,** 10338–10347
55. Katayama, T., Imaizumi, K., Sato, N., Miyoshi, K., Kudo, T., Hitomi, J., Morihara, T., Yoneda, T., Gomi, F., Mori, Y., Nakano, Y., Takeda, J., Tsuda, T., Itoyama, Y., Murayama, O., Takashima, A., St. George-Hyslop, P., Takeda, M., and Tohyama, M. (1999) *Nat. Cell. Biol.* **1,** 479–485
56. Gething, M. J. (2000) *Nat. Cell. Biol.* **2,** E21–E23